第49卷第1期 中国科学技术大学学报 Vol. 49, No. 1
2019年1月 JOURNAL OF UNIVERSITY OF SCIENCE AND TECHNOLOGY OF CHINA Jan. 2019

文章编号:0253-2778(2019)01-0079-08

Monte carlo simulation of secondary electron emission from wave-type structure

KHAN Muhammad Saadat Shakoor[1], ZOU Yanbo[1,2], LI Chao[1], DING Zejun[1]

(1. *Key Laboratory of Strongly-Coupled Quantum Matter Physics, Chinese Academy of Science, USTC, Hefei* 230026, *China*;
2. *School of Physics & Electronic Engineering, Xinjiang Normal University, Urumchi* 830054, *China*)

Abstract: Monte Carlo (MC) simulation techniques for the study of electron interaction with solids have been successfully applied to obtain the line-scan profiles in critical dimension scanning electron microscopy (CD-SEM). However, previous studies have been mostly concerned about the sample of simple geometries having sharp edges. The simulation was extended to the study of wave-type structures with smooth curved shapes. The MC model is based on using the Mott cross-section for electron elastic scattering and the full Penn algorithm in a dielectric function approach to electron inelastic scattering. The CD-SEM line-scan profiles of wave-type structures have been calculated by taking into account such experimental factors as primary beam energy, geometry parameters and material property. It is shown that by decreasing the height of the structure, the double side peaks can shrink to merge into a single peak. This characteristic will pose a challenge to the CD characterization for the smoothed line structure.

Key words: SEM, Monte Carlo, secondary electrons

CLC number: TN4, O59, O24 **Document code**: A doi:10.3969/j.issn.0253-2778.2019.01.011

Citation: KHAN Muhammad Saadat Shakoor, ZOU Yanbo, LI Chao, et al. Monte carlo simulation of secondary electron emission from wave-type structure[J]. Journal of University of Science and Technology of China, 2019, 49(1): 79-86.
KHAN Muhammad Saadat Shakoor, 邹艳波, 李超, 等. 波型结构样品二次电子发射的 Monte Carlo 模拟[J]. 中国科学技术大学学报, 2019, 49(1): 79-86.

波型结构样品二次电子发射的 Monte Carlo 模拟

KHAN Muhammad Saadat Shakoor[1], 邹艳波[1,2], 李 超[1], 丁泽军[1]

(1. 中国科学院强耦合量子材料物理重点实验室, 中国科学技术大学, 安徽合肥 230026;
2. 新疆师范大学物理与电子工程学院, 新疆乌鲁木齐 830054)

摘要: 用于研究电子与固体相互作用的 Monte Carlo(MC)模拟技术已成功应用于获得测长扫描电子显微镜(CD-SEM)中的线扫描轮廓曲线. 以前的研究主要关注具有尖锐边缘的简单几何形状的样品, 为此将相应的

Received: 2018-04-09; **Revised**: 2018-09-27

Foundation item: Supported by the National Natural Science Foundation of China(11574289), Special Program for Applied Research on Supercomputation of the NSFC-Guangdong Joint Fund (U1501501), "111" Project of the Education Ministry and Fundamental Research Funds for the Central Universities (WK6030000088).

Biography: KHAN Muhammad Saadat Shakoor, male, born in 1988, Master candidate. Research field: Physical electronics. E-mail: saadat@mail.ustc.edu.cn

Corresponding author: DING Zejun, PhD/Professor. E-mail: zjding@ustc.edu.cn

模拟扩展到具有平滑弯曲形貌的波形结构样品. MC模拟模型用Mott截面描述电子的弹性散射以及基于完全Penn算法的介电函数理论描述电子的非弹性散射. 综合考虑了不同实验因素,如电子束能量,几何参数和材料性质对波型结构样品CD-SEM线扫描曲线的影响;计算表明,随着样品结构高度的降低,二次电子的两个侧边峰可以合并成一个中心单峰,该特征为平滑线状结构样品的关键尺寸表征带来了新的挑战.

关键词: 扫描电子显微镜;Monte Carlo;二次电子

0 Introduction

Introduction

The technology and metrology of new microelectronic materials are playing a very important role in the research and development of upcoming semiconductor manufacturing. The most critical challenge will be the measurement of dimensions like critical dimension (CD) and film thickness[1]. For this, critical dimension scanning electron microscopy (CD-SEM) has been a conventional tool for measurement of CDs of nanostructures in the integrated circuit industry due to its high resolution and high efficiency[2]. Usually, line width is evaluated from line-scan profiles of secondary electron image with an empirical method, as the sharp line structure will present an edge bloom of the intensity due to the edge effect of secondary electron emission[3]. However, at nanometer scale the CD measurement needs a stricter requirement on the measurement uncertainty than the expanding of the bloom region; therefore, a model-based library (MBL) method based on Monte Carlo (MC) simulations has been proposed to cope with the challenge[4-9].

Monte Carlo (MC) simulation techniques in electron spectroscopy and scanning electron microscopy have been in use for decades[10-12]. A lot of work in both theoretical and experimental fields has been done aiming at more accurate estimation of the CD by using MC simulation. The bias of line width depends on many experimental parameters, including electron beam (primary energy, beam diameter and focusing), sample structure (structural shape and related parameters, e.g. line top and bottom widths, line height, sidewall angles, top rounding and footing for a trapezoidal line structure). However, previous studies have been entirely focused on the sample of simple geometries having sharp edges, like trapezoidal line, prepared by the etching technique. While for other line nanostructures, for example the smooth line structure prepared by an atomic deposition technique, the structural shape is a smoothly varied curve and has no sharp edges. Then the corresponding line-scan profiles of secondary electrons in an SEM image will be significantly different from the case of a trapezoidal line structure. In this work, we will present a primary study on the line-scan behavior of these line structures. Firstly, the wave-type structure is constructed with the aid of computer graphic technique. A finite element triangulated mesh is constructed by using Gmsh, a freely available GNU (general public license) meshing software[13]; combined with a spatial subdivision method the MC simulation of CD-SEM image can be accelerated[7,14-15]. It is shown that the shape of line-scan profile of secondary electron images for the wave-type structure can be changed from two side peaks to a single peak, depending on the experimental factors and mainly the height of the structure.

1 Simulation Method

1.1 Simulation Model

Monte Carlo calculation of SEM image is based on the simulation of incident electron trajectories and the generated secondary electron trajectories inside the solid target by a random sampling technique for electron scattering events including elastic scattering and inelastic scattering. The present simulation is based on MC simulation models[12,16]. Instead of using Penn's single-pole

approximation dielectric function[17], we will use the full Penn's algorithm[18] for the calculation of electron inelastic mean free paths. To calculate the electron step length, a ray tracing technique is used[14].

1.2 Electron Elastic Scattering

In order to deal with the electron elastic scattering, the Mott's cross-section[19] with the Thomas-Fermi-Dirac atomic potential is used,

$$\frac{d\sigma_e}{d\Omega} = |f(\theta)|^2 + |g(\theta)|^2 \tag{1}$$

where the scattering amplitudes,

$$f(\theta) = \frac{1}{2ik}\sum_{l=0}^{\infty}\{(l+1)(e^{2i\delta_l^+}-1) + l(e^{2i\delta_l^-}-1)\}P_l(\cos\theta) \tag{2}$$

$$g(\theta) = \frac{1}{2ik}\sum_{l=1}^{\infty}\{-e^{2i\delta_l^+} + e^{2i\delta_l^-}\}P_l^1(\cos\theta) \tag{3}$$

are calculated by partial wave expansion method[20], where δ_l^+ and δ_l^- are spin up and spin down phase shifts of the l^{th} partial wave, respectively; $P_l(\cos\theta)$ and $P_l^1(\cos\theta)$ are the Legendre and the first order associated Legendre functions, respectively.

1.3 Electron Inelastic Scattering

An electron moving inside a sample interacts with other constituting charged particles through Coulomb's interaction. Any change in the energy of a moving electron causes the excitation of the internal electrons, and hence the loss of energy of moving electron. Such an event is known as inelastic scattering. The excitation of internal electrons two modes: single particle excitation and plasmon excitation.

In a dielectric function approach to electron inelastic scattering, the differential cross section is calculated according to Penn's algorithm[17]. The algorithm is quite useful because of its wide applicability for various materials; with the use of experimental optical constants, the calculation is much more accurate for realistic materials. The double differential scattering cross section is expressed in terms of energy loss function, $\mathrm{Im}\{-1/\varepsilon(q,\omega)\}$, as

$$\frac{d^2\lambda_{in}^{-1}}{d(\hbar\omega)dq} = \frac{1}{\pi a_0 E}\mathrm{Im}\left\{\frac{-1}{\varepsilon(q,\omega)}\right\}\frac{1}{q} \tag{4}$$

where a_0 is Bohr radius, $\hbar\omega$ is energy loss, $\hbar q$ is the momentum transfer, E is the kinetic energy of moving electron, $\varepsilon(q,\omega)$ is a dielectric function of solid and λ_{in}^{-1} is the electron inelastic mean free path. In order to calculate the energy loss function, we have used the full Penn algorithm (FPA)[18] instead of the conventional single-pole approximation (SPA). The energy loss function is expanded as follows:

$$\mathrm{Im}\left\{\frac{-1}{\varepsilon(q,\omega)}\right\} = \int_0^{\infty} g(\omega_p)\,\mathrm{Im}\left\{\frac{-1}{\varepsilon_L(q,\omega;\omega_p)}\right\}d\omega_p \tag{5}$$

where $g(\omega_p)$ is the expansion coefficient which is obtained from optical energy loss function as $g(\omega) = (2/\pi\omega)\,\mathrm{Im}\{-1/\varepsilon(\omega)\}$, $\varepsilon_L(q,\omega;\omega_p)$ is Lindhard dielectric function of free electron gas having plasmon energy $\hbar\omega_p$. Since $\varepsilon(\omega)$ is related to optical constants which have been experimentally measured in a wide photon energy range and for a variety of materials[21-22], the differential cross section can be calculated conveniently and its integration leads to energy loss distribution and angular distribution for the MC simulation.

1.4 Geometrical Representation

3D specimen structure modelling and optimization of the simulation are two main aspects concerned in a 3D MC simulation for a complex geometry structure and hence, it is essential to CD metrology by the MBL method. Frase et al[6] have reviewed the available Monte Carlo simulators for the simulation of secondary electron images and described how the MBL method can be used to test and authenticate the CD metrology algorithms. Various kinds of 3D structural modelling have been proposed in the recent years. The geometric structure used in this work is mainly based on our previous works[7,15]. For geometrical structure description various approaches, like constructive solid geometry[23-25], finite element triangular mesh[7,14-15], height maps[26] and tetrahedral

mesh[27] have been used. Here we have employed the finite element triangular mesh method for the construction of the wave-type structure. The reason for adopt this finite element triangular mesh method is that it is a popular method used in many 3D graphics software. When an electron trajectory penetrates into a sample surface or emits from the surface it is easier to judge intersection points of a velocity vector with a local triangular plane. In order to construct the wave-type structure having a smoothly curved surface, we should use triangles as much as possible. Hence, the computation time in an MC simulation will also be increased linearly with the number of triangles. For this reason, we have adopted an optimization technique, i. e. the space subdivision, to accelerate calculation[14]. Only those triangulated surfaces in cubes along electron velocity ray direction would be involved in the sampling procedure.

The geometric structure of a wave-type specimen is shown in Fig. 1; The structure is constructed by using Gmsh, a freely available GNU meshing software[13], as shown in Fig. 1. The structure is described by the following parameters: height H, bottom width W, bottom circular arc s_1 with angle α_1 and peak circular arc s_2 with angle α_2. In order to have a symmetry we have constructed the structure with the same parameters for the left and right sides of the structure. The structure peak is constructed by three points: the middle point is exactly at the peak top position, and the right and left points of the peak are at the end of a circular arc s_2 having angle α_2. The left and right bottoms of the structure are constructed by two points individually. The first point is at the boundary of the structure and the second point is at the end of circular arc s_1 having angle α_1. Then we have employed Gmsh software to join all these points by a spline and develop a finite element triangular mesh for modeling of a sample surface with wave-type geometry.

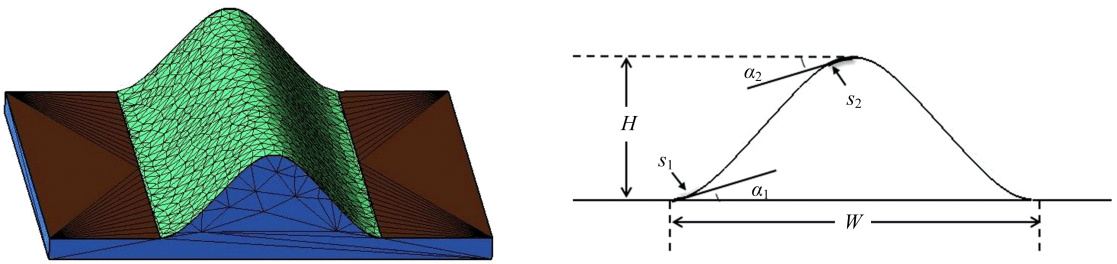

(a) Triangular mesh of a wave拟type structure (b) Schematic diagram of wave拟type structure specified by parameters

Fig. 1 The geometric structure of a wave-type specimen

1.5 Boundary Correction

In a sampling of scattering events, an important step is to determine the electron transport step length between two successive collisions. In a bulk sample case this is simple because only one material is involved in the scattering mean free path. However, for a structure made of a line placed on a substrate, different mediums are contained in different structural parts or elemental zones; the boundary correction used for the transport step length should be made. We use a ray tracing technique to determine exact electron step length passing through different elemental zones by recording the location of the intersection of velocity vector with a boundary, which is either the interface between different elemental zones or the material surface[23,28]. The step length S is calculated by

$$\sum\nolimits_i l_i/\lambda_i = -\ln R, S = \sum_i l_i \qquad (6)$$

where R is a random number, l_i is the partial step length within the ith elemental zone whose transport electron mean free path is λ_i.

Refraction of an electron trajectory at a local triangular surface is calculated in three steps: firstly, transforming the direction of an electron velocity vector from old (x,y,z) — frame of axes to a new frame of reference, (x',y',z'), having z'-axis perpendicular to a triangular plane,

$$\begin{pmatrix} v'_x \\ v'_y \\ v'_z \end{pmatrix} = \begin{pmatrix} \cos\theta_N \cos\varphi_N & \cos\theta_N \sin\varphi_N & -\sin\theta_N \\ -\sin\varphi_N & \cos\varphi_N & 0 \\ \sin\theta_N \cos\varphi_N & \sin\theta_N \sin\varphi_N & \cos\theta_N \end{pmatrix} \begin{pmatrix} v_x \\ v_y \\ v_z \end{pmatrix} \tag{7}$$

where (v_x, v_y, v_z) and $\varphi(v_{x'}, v_{y'}, v_{z'})$ are respectively the unit vectors in the old and new frames of reference; θ_N and φ_N are polar and azimuthal angles of the surface normal vector N. Secondly, when an electron is ejected from the sample surface and enters the vacuum a quantum mechanical transmission coefficient is applied,

$$T(E_1, \vartheta_1) = \begin{cases} \dfrac{4\sqrt{1 - U/E_1 \cos^2\vartheta_1}}{(1 + \sqrt{1 - U/E_1 \cos^2\vartheta_1})^2}, & \text{if } E_1 \cos^2\vartheta > U \\ 0, & \text{otherwise} \end{cases} \tag{8}$$

Then the law of refraction is applied and the electron changes its moving direction according to $\sqrt{E_1}\sin\vartheta_1 = \sqrt{E_2}\sin\vartheta_2$, where E_1 and E_2 represent electron energies, and ϑ_1 and ϑ_2 are the polar angles of moving direction inside and outside of the solid, respectively.

2　Results and Discussion

In our previous calculations[16,18,29] satisfactory results on secondary yield and energy distribution curves along with backscattering energy spectra have been successfully obtained, which has proven the accuracy of this MC simulation. In this work we have used FPA instead of SPA for the modeling of electron inelastic scattering and the associated secondary electron excitation. The secondary yield obtained by SPA in the beam energy range of 100 eV to 2 keV is higher than that of FPA, while the secondary electron energy spectrum calculated by FPA is closer to the experimental universal curve shape than the SPA.

For simple structures having sharp edges, e. g. trapezoidal shape line structure, the signal intensity of line-scan increases significantly at an edge, which is due to the extra secondary electron emission from nearby local surfaces and called as the edge effect. While for the line structure of wave-type shape there is no such a shape edge and the SEM line-scan profiles are unknown. For this, we have simulated the line-scans for a wave-type line placed on a bulk substrate, i. e. Au/Si and Si/Si, and by changing electron beam energy and geometry parameters. Fig. 2 shows the simulation results for beam energy of 1 and 5 keV; the beam size (FWHM) is 5 nm. The bottom width of the wave structure is $W = 100$ nm; the total size of the substrate plane for the simulation is 400 nm × 400 nm. We have scanned the structure at the midpoint (200 nm) of the structural cross section so that the electron cannot escape from the side surface of the structure. The line-scan shape is very sensitive to the height of the structure, and also significant change of peak intensities have been observed with the change of the structure height. At the largest height considered, 70 nm, for both Au/Si and Si/Si samples we observed a side effect instead of an edge effect: the emission of the secondary electrons has a maximum around the mid of the side slope of the smoothly varying structure. This can be explained by the inverse cosine law, $1/\cos^n\theta$, of the angular distribution of secondary electron emission, where θ is the tilt angle between electron incident direction and local surface normal, and n varies from 1. 3 for light elements to 0. 8 for heavy elements[30]: Near the top and bottom region the local tilt angle is small, while it is the largest at the mid of slope.

By decreasing the height, the sidewall angle and hence the maximum tilt angle reduce; this results in smaller emission intensity. The peak intensity for the side peaks also decreases gradually, and finally at $H = 40$ nm for Au/Si in Fig. 2(a) and $H = 30$ nm for Si/Si in Fig. 2(b) for the primary energy of 1 keV they emerge together to become a single peak at the line center position. By further decreasing the height this top peak becomes sharper. The main reason of this sharpness is that the top peak appears at exactly the center of the structure and the heights of both sides portions of the structure are small compared

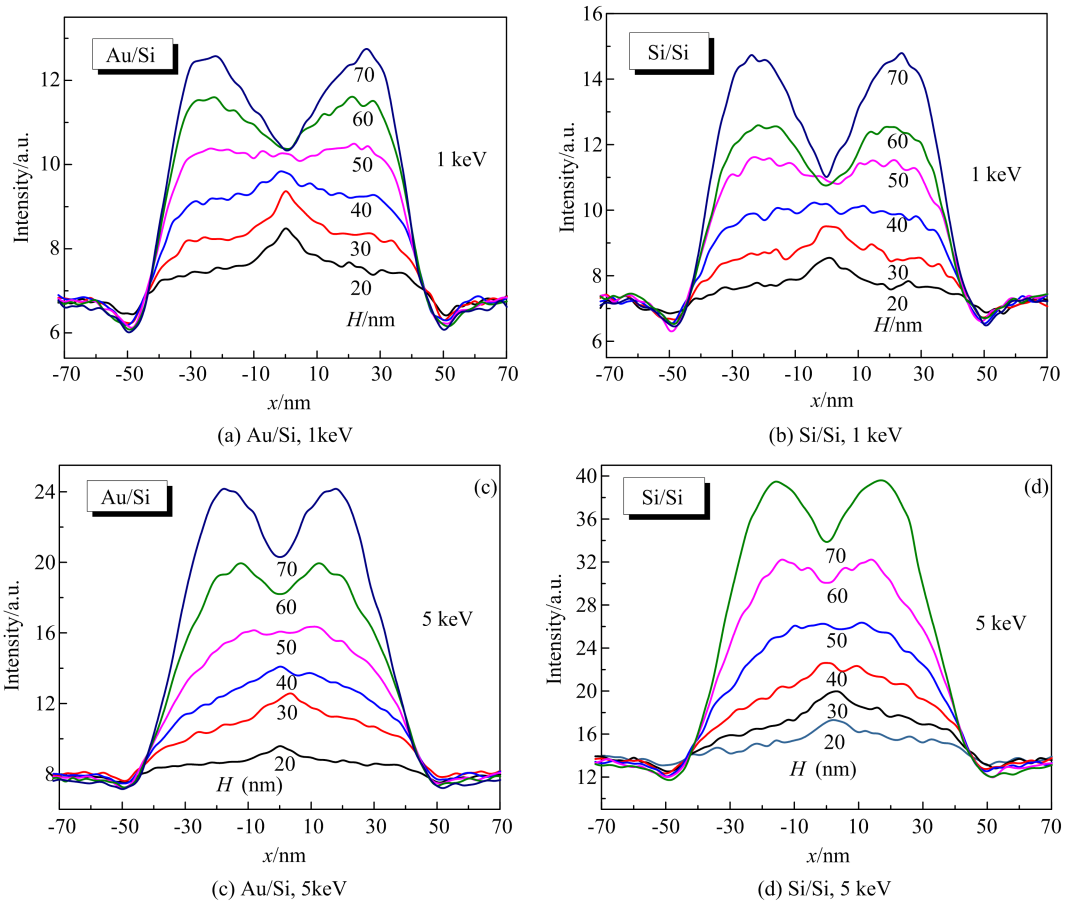

Fig. 2 MC simulation results

with the length of the structure. Two materials for the line structure, i. e. Au and Si, give a similar variation trend but in different magnitudes; this is because the secondary electron emission from Au is higher than that from Si[31] due to the larger β-factor for Au for the greater contribution from backscattered electron[32], where the β-factor is the ratio of the secondary yield per backscattered electron to the secondary yield per incident electron[33]. Although a significant number of primary electrons can penetrate from the Si substrate, and the emitted secondary electrons are almost from the very thin region under the surface[34]; hence, the substrate has played only a minor role in secondary emission intensity.

The beam energy also plays an important role in the quantitative line-scan profiles through its influence on secondary emission intensity. Figs. 2(a) and 2(c) compare the line-scans of an Au/Si wave-type specimen at primary energies of 1 keV and 5 keV, respectively; similarly, Figs. 2(b) and 2(d) compare the line-scans of a Si/Si wave-type specimen. With the increase in primary energy, the range of the intensity enhancement for the line structure is narrowed, which is related to the smaller secondary emission by backscattered electrons at higher energy because of deeper penetration into the specimen. However, the sharpness of the image or the topographic contrast of the line is blurred. Then the lower energies are more preferable for the measurement of line width via SEM image contrast.

In order to observe the effect of differentline heights on the line-scan of wave-type specimen but at smaller widths, we have performed simulation under the same conditions as in Fig. 3 but at the smaller bottom width of the wave structure, $W=$ 50 nm. Whereas the total size of the substrate plane for the simulation is 350 * 350 nm we have scanned the structure at the midpoint of 175nm. Due to the reduction of width, for the same height of line the sidewall angle is increased so that the

side peak intensity is enhanced. However, on the other hand, reducing the line width to such a small size may also reduce the secondary emission intensity.

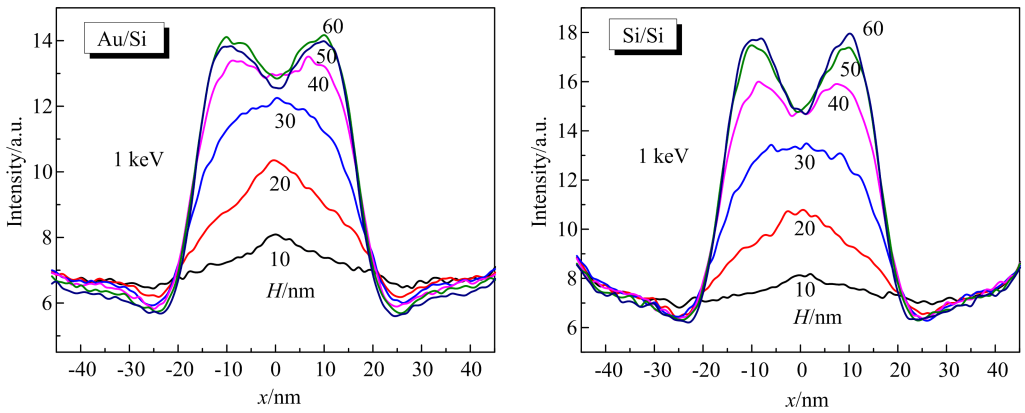

(a) Au/Si, 1keV　　(b) Si/Si, 1 keV

Fig. 3　Simulated SE line-scans of a wave-type line structure on a substrate at different heights for the bottom width of $W=50$ nm and $\alpha_1=\alpha_2=100$

There are other minor parameters that can also alter the line-scan shape, like electron beam size and focusing distance, incident angle, roughness of the structure surface, bottom and peak circular arcs. In CD-SEM the normal incidence is used but may have a slight inclined angle. Signal noise in an CD-SEM image can also produce measurement errors. The quality of focus is also important for the shape of the line-scan profile. However, the biggest measurement error of the line width will be the choice of width determination algorithm. Here in this work we have demonstrated that the signal intensity line-scan profile and the image contrast rely on many experimental parameters related to the electron beam and structure geometry. Thus, it is very hard to find a suitable analytical form for width determination. According to the methodology of MBL, a model-based algorithm should be the best way to perform an accurate 3D measurement of the trapezoidal line structure. The present example of wave-type line structure has presented an even greater challenge to the CD characterization of the smooth line shapes as their line-scan profiles of secondary electrons in a CD-SEM have no sharp edge peak behavior. MBL method is perhaps still the very necessary tool for this end.

Acknowledgement

Thanks Dr. LI Huiming and the supercomputing center of USTC for the support of parallel computing.

References

[1] VOGEL E M. Technology and metrology of new electronic materials and devices [J]. Nature Nanotechnology, 2007, 2(1): 25-32.

[2] MOROKUMA H, MIYAMOTO A, TANAKA M, et al. New technique to reconstruct effective 3D profile from tilt images of CD-SEM [C]// Proceedings of SPIE. Florida, USA: SPIE, 2004: 5375-5378.

[3] DING Z J, SHIMIZU R. Theoretical study of the ultimate resolution of SEM[J]. Journal of Microscopy, 1989,154(3): 193-207.

[4] VILLARRUBIA J S, VLADÁR A E, POSTEK M T. Scanning electron microscope dimensional metrology using a model-based library[J]. Surface and Interface Analysis, 2005, 37(11): 951-958.

[5] BABIN S, BORISOV S, LVANCHIKOV A, et al. Calibration of CD-SEM: Moving from relative to absolute measurements [C]// Proceedings of SPIE. Guangzhou, China: SPIE, 2008: 6922(1-8).

[6] FRASE C G, GNIESER D, BOSSE H. Model-based SEM for dimensional metrology tasks in semiconductor and mask industry[J]. Journal of Physics D: Applied Physics, 2009, 42(18): 189001(1-17).

[7] LI Y G, ZHANG P, DING Z J. Monte Carlo simulation of CD-SEM images for linewidth and critical dimension metrology [J]. Scanning, 2013, 35(2):

127-139.
[8] VLADÁR A E, VILLARRUBIA J S, CHAWLA J, et al. 10nm three-dimensional CD-SEM metrology[C]// Proceedings of SPIE. San Jose, USA: SPIE, 2014: 90500A(1-11).
[9] ZOU Y B, KHAN M S, LI H M, et al. Use of model-based library in critical dimension measurement by CD-SEM[J]. Measurement, 2018, 123:150-162.
[10] SHIMIZU R, DING Z J. Monte Carlo modelling of electron-solid interactions[J]. Report on Progress in Physics, 1992, 55(4): 487-531.
[11] JOY D C. Monte Carlo Modeling for Electron Microscopy and Microanalysis [M]. New York: Oxford University Press,1995a.
[12] DING Z J, SHIMIZU R. A Monte Carlo modelling of electron interaction with solids including cascade secondary electron production[J]. Scanning, 1996, 18 (2): 92-113.
[13] GEUZAINE C, REMACLE J F. Gmsh: A 3-D finite element mesh generator with built-in pre-and post-processing facilities [J]. International Journal for Numerical Methods in Engineering, 2009, 79(11): 1309-1331.
[14] LI Y G, MAO S F, LI H M, et al. Monte Carlo simulation study of scanning electron microscopy images of rough surfaces [J]. Journal of Applied Physics, 2008, 104(6): 064901(1-7).
[15] ZHANG P, WANG H, LI Y G, et al. Monte Carlo simulation of secondary electron images for real sample structures in scanning electron microscopy [J]. Scanning, 2012, 34(3): 145-150.
[16] DING Z J, TANG X D, SHIMIZU R. Monte Carlo study of secondary electron emission[J]. Journal of Applied Physics, 2001, 89(1): 718-726.
[17] PENN D R. Electron mean-free calculations using a model dielectric function [J]. Physical Review B, 1987, 35(2): 482-486.
[18] MAO S F, LI Y G, ZENG R G, et al. Electron inelastic scattering and secondary electron emission calculated without the single pole approximation[J]. Journal of Applied Physics, 2008, 104(11): 114907(1-10).
[19] MOTT N F. The scattering of fast electrons by atomic nuclei[J]. Proceedings of the Royal Society of London A, 1929, 124(794): 425-442.
[20] YAMAZAKI Y. Studies on electron scattering by mercury atoms and electron spin polarization detector [D]. PhD Thesis, Osaka University, 1977.
[21] PALIK E D. Handbook of Optical Constants[M]. London: Academic Press, 1985.
[22] HENKE B L, GULLIKSON E M, DAVIS J C. X-ray interactions: Photo absorption, scattering, transmission, and reflection at $E = 50$-30000 eV, $Z = 1-92$[J]. Atomic Data and Nuclear Data Tables, 1993, 54(2): 181-342.
[23] DING Z J, LI H M. Application of Monte Carlo simulation to SEM image contrast of complex structures[J]. Surface and Interface Analysis, 2005, 37(11): 912-918.
[24] LI H M, DING Z J. Monte Carlo simulation of secondary electron and backscattered electron images in scanning electron microscopy for specimen with complex geometric structure[J]. Scanning, 2005, 27 (5): 254-267.
[25] YUE Y T, LI H M, DING Z J. Monte Carlo simulation of secondary electron and backscattered electron images for a nanoparticle-matrix system[J]. Journal of Physics D: Applied Physics, 2005, 38(12): 1966-1977.
[26] VALLARRUBIA J S, VLADÁR A E, MING B, et al. Scanning electron microscope measurement of width and shape of 10nm patterned lines using a JMONSEL-modeled library [J]. Ultramicroscopy, 2015, 154: 15-28.
[27] VILLARRUBIA J S, VLADÁR A E, POSTEK M T. 3D Monte Carlo modeling of the SEM: Are there applications to photomask metrology[C]// Proceedings of SPIE. 2014: 923602(1-12).
[28] CLEARY J G, WYVILL G. Analysis of an algorithm for fast ray tracing using uniform space subdivision[J]. The Visual Computer,1988,4(2): 65-83.
[29] DING Z J, LI H M, TANG X D, et al. Monte Carlo simulation of absolute secondary electron yield of Cu [J]. Applied Physics A, 2004, 78(4): 585-587.
[30] REIMER L. Scanning Electron Microscopy-Physics of Image Formation and Microanalysis[M]. 2ed, Berlin: Springer, 1998.
[31] JOY D C. A database on electron-solid interactions[J]. Scanning, 1995, 17(1): 270-275.
[32] CAZAUX J. About the role of the various types of secondary electrons (SE1; SE2; SE3) on the performance of LVSEM[J]. Journal of Microscopy, 2004, 214(3): 341-347.
[33] JOY D. A model for calculating secondary and backscattered electron yields [J]. Journal of Microscopy, 1987, 147(1): 51-64.
[34] ZOU Y B, MAO S F, DA B, et al. Surface sensitivity of secondary electrons emitted from amorphous solids: Calculation of mean escape depth by a Monte Carlo method[J]. Journal of Applied Physics, 2016, 120 (23): 235102-1-12.